

First-principles study of hydrogen absorption on Mg(0001) and formation of magnesium hydrideTao Jiang,^{1,2} Li-Xian Sun,² and Wei-Xue Li^{1,*}¹*State Key Laboratory of Catalysis, and Center of Theoretical and Computational Chemistry, Dalian Institute of Chemical Physics, Chinese Academy of Sciences, Dalian 116023, China*²*Laboratory of Aerospace Catalysis and New Materials, Dalian Institute of Chemical Physics, Chinese Academy of Sciences, Dalian 116023, China*

(Received 23 August 2009; revised manuscript received 22 November 2009; published 15 January 2010)

The hydrogen absorption on Mg(0001) surfaces, penetration into the subsurface region, and transition toward magnesium hydride up to six monolayer absorption is studied by density-functional theory calculations. The favorable absorption sites are identified, and average absorption energies and their dependence on the coverage are calculated and analyzed by projected density of states. It is found that at lower absorption (less than one monolayer), H atoms prefer to adsorb at on-surface fcc sites, and the bonding strength increases with the absorption due to the enhanced hybridization between H and Mg substrates. We find that the H absorption in the subsurface region is energetically unfavorable until full monolayer H absorption on the Mg(0001) surfaces. After this, H absorption in the subsurface region becomes energetically and kinetically favorable, and forms a stable locale H-Mg-H trilayer (so-called surface hydride with local uptake of two monolayers). It is found that the H-Mg-H trilayers interact weakly with Mg substrates underneath and grow steadily by stacking with each other at constant average absorption energy. The H-Mg-H trilayers is proposed to be the precursors of the formation of magnesium hydride. It is found that when the number of the H-Mg-H trilayers is over three (six monolayer for overall uptake), the transition to the MgH₂(110) would be energetically favorable.

DOI: [10.1103/PhysRevB.81.035416](https://doi.org/10.1103/PhysRevB.81.035416)

PACS number(s): 68.43.-h, 82.65.+r, 68.35.Md

I. INTRODUCTION

Hydrogen is considered to be an ideal energy carrier for its abundance in nature, high energy efficiency, and environmental friendliness. Realization of the hydrogen economy depends on three critical steps: production, storage, and application. Among of these, hydrogen storage with appropriate thermodynamics, fast kinetics (quick uptake and release), and high gravimetric and volumetric densities (light in weight and conservative in space)¹ has to be met, especially for the use of hydrogen as fuel for on board application. The applicability of metal hydrides as potential hydrogen storage material has been studied intensively. Due to the hydrogen gravimetric capacity of up to 7.7% and low cost of magnesium, it is thought as one of the promising candidates to meet the goal of automotive application.^{2,3} The challenges remained is its slow kinetics for hydrogen uptake and high thermodynamic stability of MgH₂ formed. To improve the performance of Mg as hydrogen storage material, extensive studies have been conducted, mainly focused on two routes: (1) adding and/or alloying transition metals particles with magnesium to lower dissociation barrier of hydrogen molecules hydride,⁴⁻⁸ and (2) decreasing Mg particle size downwards to nanoscale with and without additive to destabilize the magnesium hydride.⁹ Though the kinetics for hydrogen uptake and releases has been improved continuously, for instance, temperatures for hydrogen uptake and release on Mg alloy can be reduced as lower as 423 and 573 K, respectively. In this temperature, typically the uptake of the hydrogen takes about one hour.⁷ These are still far behind the requirement for practical applications, where operating temperatures should be less than 323 K, H filling should be finished in few minutes.¹ To shed lights on these, microscopic study and understanding is required.

Ultrahigh vacuum (UHV) study on hydrogen absorption on Mg(0001) surfaces is limited by the significant barrier for hydrogen dissociations and lower sublimation temperature of Mg (423 K).^{10,11} At earlier 1990s, Sprunger and Plummer studied the hydrogen absorption on Mg(0001) surfaces using electron energy lost spectrum (EELS), where hydrogen molecules were cracked to atomic hydrogen by a hot W-filament doser.^{12,13} They found that for molecular hydrogen absorption, there is a chemisorbed precursor state; while for atomic hydrogen absorption, it was suggest that absorption at three-fold hollow sites was preferred. Higuchi *et al.*¹⁴ investigated the hydrogen absorption on well prepared Pd/Mg/Pd sandwiches and found that hydriding and dehydriding properties have been improved significantly, which were attributed to interfacial strain. Recently, Ostefeld and co-workers investigated absorption as well as desorption properties of hydrogen on clean and platinum (Pt) modified magnesium films grown on the molybdenum substrate.^{10,11} It was found that on pure Mg films, the rate of hydrogen uptake decreases with time, and total uptake amount saturates at 2.5 monolayer (ML) in 50 min when temperature is lower than 423 K. The reason was attributed to formation of dense hydrogen overlayer with a considerable heat of absorption self blocking the hydrogen diffusion into the film. While for Pt modified films, hydrogen uptake reaches 6 ML within one hour under room temperature without decreasing on uptake rate; at 348 K, hydrogen uptake can easily go to more than 15 ML within 1500 s. The reason was attributed to the catalytic role and weakened influence of self blocking caused by the adsorbed hydrogen by added Pt.

Theoretical studying of H₂ dissociation on Mg(0001) was first reported by Norskov and Houmøller using jellium model 80s, where a chemisorbed precursors state of H₂ was found.¹⁵ H₂ dissociation on Mg(0001) surfaces was studied recently by Vegge¹⁶ using density-functional theory calcula-

tions and revised Perdew-Burke-Ernzerhof (RPBE) (Ref. 17) functional, and a significant barrier 1.15 eV was obtained in this work. Furthermore, it was found that at coverage of 0.25 ML, the barrier for the penetration of hydrogen atom from the surface into the subsurface and bulk region through fcc channel was 0.53 and 0.18 eV, respectively. Similar results were reported recently by Jacobson *et al.*¹⁸ and Wu *et al.*¹⁹ These works indicate that hydrogen dissociation is the rate-limiting step, and hydrogen diffusion in the magnesium bulk is facile. The hydrogen dissociation on transition metal doped Mg surface and Mg surface with carbon atoms incorporation in subsurface were calculated by Du and co-workers, where the calculated barrier is 0.10 and 0.89 eV, respectively.^{20,21} Wagemans and co-workers have calculated the energies of Mg and MgH₂ clusters, and their results show that MgH₂ is destabilized significantly which may translates to a lower hydrogen desorption temperature for these small MgH₂ clusters.²²

Though valuable insights were obtained from these studies, theoretical studies conducted so far focus mainly on the interactions between magnesium and hydrogen at lower coverage (less than 0.25 ML). Hydrogen absorption, diffusion into the subsurface and bulk region as well as the formation of the magnesium hydride involves significant amount of hydrogen, which is however far beyond the submonolayer regime. Particularly, the microscopic understanding of hydrogen absorption at high coverage and the transition to the metal hydride, which is crucial to improve the kinetics of hydrogen uptake, is remaining. In the present work, we report a systematic density-functional theory (DFT) study on the H absorption on Mg(0001) at range of the coverage up to 4 ML. Atomistic evolution from chemisorption, penetration into the subsurface region, to the formation metastable precursor state of H-Mg-H trilayer toward the transition of the magnesium hydride are first mapped out. The remaining paper is organized as follows: in Sec. II, the details of calculation method are presented. The hydrogen absorption on Mg(0001) surfaces at coverage up to 1 ML are studied in Sec. III. Hydrogen diffusion into the subsurface region and formation of H-Mg-H trilayer (surface hydride) are presented in Sec. IV, and subsequently formation of the multi trilayers is studied in Sec. V. Finally, conclusion is given in Sec. VI.

II. CALCULATION METHODS

DFT calculations are performed using highly optimized package DACAPO,¹⁷ in which ultrasoft pseudopotentials are used to describe the interaction between valence and core electron,²³ and the wave functions are expanded in plane waves with an kinetic energy cutoff of 350 eV. To describe electron exchange-correlation interaction, generalized gradient approximation with Perdew-Wang 91 (PW91) functional is adopted. The magnesium surface Mg(0001) is modeled by a five-layer-slab separated by 12 Å of vacuum; hydrogen atom is placed on one side of the slab, where the induced dipole moment is taken into account by applying a dipole correction.²⁴ The adsorbed hydrogen atoms and top most three Mg layers are fully relaxed until the forces on the atoms are less than 0.02 eV/Å, as well as the clean Mg sur-

face. Test calculations showed that the adsorbated-substrates system has negligible spin and nonspinpolarization calculations are conducted throughout the present work. A (4 × 4 × 1) Monkhorst-Pack grid²⁵ is used to sample the Brillouin zone of (2 × 2) Mg(0001) surface. We employ a Fermi function with a temperature broadening parameter of $k_B T = 0.15$ eV (where k_B is the Boltzmann constant) to improve the convergence, and the resulted total energies are extrapolated to zero temperature to calculate the energetics.

The average (dissociative) absorption energy E_{ab} per hydrogen atom with respect to the hydrogen molecule in gas phase, is calculated by

$$E_{ab} = \frac{1}{N_H} \left[E_{H/Mg(0001)} - \left(E_{Mg(0001)} + \frac{1}{2} N \times E_{H_2} \right) \right], \quad (1)$$

where N is the total number of hydrogen atoms of the absorption system, and $E_{H/Mg(0001)}$, $E_{Mg(0001)}$, and E_{H_2} are total energies of the optimized H-Mg systems, the clean Mg slab and H₂ in gas phase, respectively. It is defined such that a negative E_{ad} indicates that the absorption is exothermic (stable) with respect to H₂ in gas phase, and positive is endothermic (unstable).

For bulk hcp Mg, the calculated lattice constants are $a = 3.21$ Å and $c/a = 1.62$, which agree well with full-potential linearized augmented plane-wave (FP-LAPW) result ($a = 3.20$ Å and $c/a = 1.62$).²⁶ Using ultrasoft pseudopotential plane-wave method, Vegge¹⁶ and Du *et al.*²⁰ reported similar lattice constant ($a = 3.19$ Å) by RPBE and PBE functionals, respectively. The calculated bulk modulus B is 0.34 MBar. All these results are in-line with experimental measurements, $a = 3.21$ Å, $c/a = 1.624$, and $B = 0.35$ MBar.²⁷ Calculated cohesive energy of hcp Mg is -1.50 eV, while FP-LAPW gives -1.77 eV (local density approximation) and -1.50 eV (PBE),²⁶ respectively, which agree well with experimental measurement -1.51 eV.²⁷ For clean Mg(0001) surfaces, calculated work function is 3.72 eV, which is inline with experimental value of 3.66 eV.²⁸ For isolated H₂ molecule in a cubic cell of side length 12 Å with single k point, calculated binding energy of H₂ is -4.55 eV, the bond length $d = 0.75$ Å, and the vibrational frequency $\omega = 4414$ cm⁻¹, corresponding to a zero-point energy (ZPE) of 0.273 eV, which are in excellent agreement with experimental and previous calculations.^{16,29} All these results show that the present setups provide reliable description for H-Mg systems.

We note that the ZPE is neglected in present work. The possible error bar is however estimated here. For gas phase H₂, bulk Mg and MgH₂, calculated ZPE were 0.135 eV/H atom, 0.015 eV/Mg atom, and 0.200 eV/H atom, respectively.³⁰ While, for H dissociative adsorption on Mg(0001) surfaces, calculated ZPE for H-Mg vibration was 0.137 eV/H atom.¹⁶ From these, it can be found that for the H dissociative adsorption on Mg(0001), the error bar by neglecting ZPE is 0.002 eV taking into account of the ZPE cancellation of Mg substrates before and after H adsorption, while for the formation of bulk MgH₂, the error bar is 0.050 eV/H atom. Namely, the absolute absorption energies (calculated) by neglecting ZPE in present work is therefore overestimated by 0.050 eV/H atom in maximum. The relative

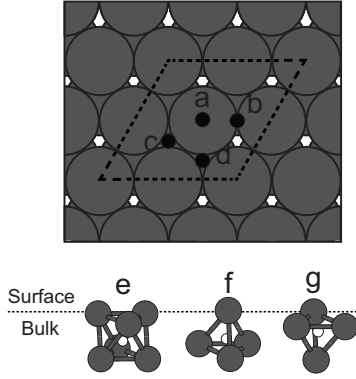


FIG. 1. Hydrogen absorption sites on Mg(0001). The upper plot is the top view of Mg(0001) surface and different absorption sites are indicated: a, b, c, and d represent on-surface top, bridge, fcc, and hcp hollow sites, respectively. The lower three plots are the side views for possible subsurface H sites below the first Mg layer, which are (e) octa, (f) tetraI, and (g) tetraII, respectively. The dashed line shows the surface unit cell used in the calculation.

difference between various absorption structures would be even less.

The dependence of the calculations on the exchange-correlation functional (PW91 and RPBE) has been checked in the present works. Test calculations show that compared to RPBE, the average absorption energy from PW91 is slightly overestimated by ca. 0.15 eV at maximum. The variation in the relative difference between various structures considered is however less than 0.03 eV. Hence both exchange-correlation functionals give same trend, and will not influence our conclusions. Increase in the thickness of the slab from five to six layers, the absolute value of the absorption energy increases only 0.01 eV/H atom. Recently, Liang studied carefully the dependence of the binding energy of H adsorption on Mg(0001),³⁰ and found that the difference of the absolute binding energy for H adsorption on six layers Mg(0001) with respect to the eighteen layers Mg(0001) is 0.07 eV/H atom. In this context, we note that though absolute binding energetics is important, the relative difference between various absorption structures, which is essential to the relative stability as the main focus in the present work, is described more reliable due to the error cancellation. We therefore conclude that the present setup gives a reliable description to the present work, and our main conclusion is less affected.

III. HYDROGEN ADSORPTION ON AND BELOW Mg(0001) ($\theta \leq 1$ ML)

A. Hydrogen absorption on Mg(0001)

Hydrogen absorption on the Mg(0001) surface at ($\theta \leq 1$ ML) is studied in this section. Various absorption sites: top, bridge, fcc, and hcp hollow, are considered. Our calculations show that hydrogen absorption at bridge and top sites are unstable and it displaces automatically to the hollow sites nearby. Therefore, only absorptions at fcc- and hcp hollow sites, shown schematically in Fig. 1, are discussed below. Calculated average absorption energies E_{ad} , for cover-

TABLE I. Calculated average absorption energy (eV) for pure on-surface fcc and hcp hollow site hydrogen at coverage less than 1 ML.

θ	0.25 ML	0.50 ML	0.75 ML	1.00 ML
fcc	-0.05	-0.10	-0.15	-0.19
hcp	-0.02	-0.05	-0.07	-0.10

age from 0.25 to 1 ML are list in Table I and plotted in Fig. 2. We find that H absorption at fcc hollow sites are energetically favorable than hcp hollow sites in the range of coverage considered (≤ 1 ML), though the difference is modest and less than 0.1 eV. The site preference found agrees with Jacobson's calculations.¹⁸ Furthermore, for both fcc and hcp hollow sites, the absorption energies decrease (absolute absorption energy becomes larger) with the coverage up to one monolayer. This shows that the bonding strength between adsorbates and substrates increases with the coverage, which will be discussed further below.

Calculated projected density of states (PDOS) for clean and H-covered Mg(0001) surface are plotted in Fig. 3. For clean Mg(0001) surface [Fig. 3(a)], it can be seen that both of Mg 3s and 3p bands were (partially) occupied above -6 eV. Mg 3s band prevails mainly at low energy range around -5 eV, while 3p band locates mainly at high energy range around -1 eV. Hybridization between 3s and 3p bands are also recognized. These agree well with previous theoretical calculations.³¹⁻³³ For H-covered surfaces at $\theta = 0.25$ ML, 0.50, 0.75, and 1.00 ML, PDOS for adsorbed H and surface Mg bonded with H are plotted in Figs. 3(b)-3(e), respectively. At low coverage of 0.25 ML, H 1s orbital hybridizes mainly with Mg 3s band at low lying level. With increase in the coverage, the hybridization with Mg 3p band at high lying level increases gradually. Increase in the hybridization between adsorbed H atoms and surface Mg atoms with coverage, rationalizes the enhanced interaction between H and Mg surfaces as found from above energetics.

B. Isolated subsurface hydrogen

For H absorption below the surfaces, there are three possible interstitial sites available, which are schematically plot-

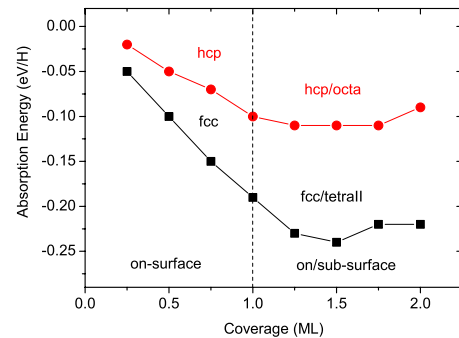


FIG. 2. (Color online) Calculated absorption energy for H on fcc (square) and hcp (circle) sites at coverage less than 1 ML and favorable structures with presence of both on-surface and subsurface hydrogen fcc/tetraII and hcp/octa (see details in the main context) at coverage from 1 to 2 ML. The solid lines are used to guide the eye.

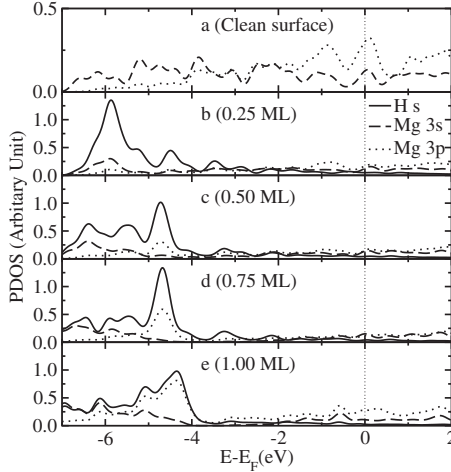


FIG. 3. (a) PDOS for Mg atoms for clean surface, and adsorbed H atoms (solid line) and surface Mg atoms 3s (dash line) and 3p (dot line) bands at (b) 0.25, (c) 0.50, (d) 0.75, and (e) 1.00 ML, respectively.

ted in Figs. 1(e)–1(g): (i) octahedral sites (noted as octa), which has six nearest-neighbor Mg atoms (three above and three below), and (ii) tetrahedra sites I (tetraI), which has four nearest-neighbor Mg atoms (one on top and three below with respect to normal direction of surface); (iii) tetrahedra sites II (tetraII) (three Mg atoms above and one right below). For the hydrogen absorption below the topmost Mg layer, octa H sits directly below on-surface fcc sites, while tetraII H sits right below on-surface hcp sites.

We found that the absorption of the isolated subsurface H at 0.25 and 0.33 ML was energetically either unstable or endothermic. This tells that at low coverage (less than 0.33 ML), dissociative hydrogen atom tends to stay on the surfaces. To study the bulk dissolved hydrogen at low coverage, we calculate a $(4 \times 4 \times 4)$ bulk Mg with one H atom placed at octa and/or tetra sites. The structures have been fully optimized, and calculated absorption energies are 0.22 eV for octa and 0.10 eV for tetra, respectively; namely, the absorption is still endothermic and energetically unfavorable. However, since there are a vast number of sites available in the bulk and the contribution from the configuration entropy would become significant, certain amount of H dissolved in the bulk is likely.

At higher coverage with preadsorbed hydrogen on the surface, H atoms may absorb in the subsurface region. To study this, we consider first the structures at 0.25 ML H on the surface ($\theta_{\text{on}}=0.25$ ML) and 0.25 ML H in the subsurface sites ($\theta_{\text{sub}}=0.25$ ML) in a (2×2) supercell with overall absorption $\theta_{\text{total}}=0.50$ ML. Three possible sites: octa, tetraI, and tetraII for subsurface H atoms, which share at least one surface Mg atom bonded with on-surface H atom, were studied and schematically shown in Fig. 1. Calculated absorption energies (Table II) are 0.08, -0.04 , and -0.03 eV, respectively, compared to the -0.10 eV when both H atoms adsorb on the surface fcc sites (Table I). Adding another 0.25 ML of hydrogen on the surface (now $\theta_{\text{on}}=0.50$ ML and $\theta_{\text{total}}=0.75$ ML), calculated absorption energies are 0.02, -0.04 , and -0.12 eV, respectively. Their energetics are still higher

TABLE II. Calculated average absorption energy (eV) for the structures with mixed subsurface (octa, tetraI, and tetraII) [$(\theta_{\text{sub}}=0.25$ ML)] and on-surface fcc ($\theta_{\text{on}}=0.25, 0.50$, and 0.75 ML) hydrogen. The total coverage (θ_{total}) is indicated at the bottom.

Subsurface (ML)	On-surface fcc (ML)		
$\theta_{\text{sub}}=0.25$	$\theta_{\text{on}}=0.25$	$\theta_{\text{on}}=0.50$	$\theta_{\text{on}}=0.75$
octa	0.08	0.02	-0.06
tetraI	-0.04	-0.04	-0.07
tetraII	-0.03	-0.12	-0.19
θ_{total}	0.50	0.75	1.00

than pure on-surface H absorption ($\theta_{\text{total}}=\theta_{\text{on}}=0.75$ ML) with the absorption energy of -0.15 eV. This is true even additional 0.25 ML H is placed on the surface with overall absorption up to 1 ML (bottom of Table. II), though the difference between pure on-surface absorption and coabsorption structure is almost degenerate and falls in the numerical error. These calculations show clearly that for H absorption θ_{total} up to 1 ML, H prefers energetically to stay on the surface fcc sites. At higher coverage, H atoms start to adsorb at the subsurface tetraII sites.

IV. FORMATION OF H-Mg-H TRILAYER ($1 \text{ ML} \leq \theta \leq 2 \text{ ML}$)

The hydrogen penetration into the subsurface and bulk region is critical for the transition and formation of the magnesium hydride. In literatures, hydrogen penetration into the subsurface region of Mg(0001) has been studied by Vegge¹⁶ using DFT. In this work, a barrier for diffusion through surface Mg layer, 0.53 eV, was obtained, and further diffusion into the bulk with barrier of 0.18 eV was found to be a facile process and not rate-limiting step. In this work, the calculations were done in (2×2) cell with one hydrogen atom. Namely, only hydrogen diffusion at low coverage was considered. To study the hydrogen absorption into the subsurface region at high coverage, we considered a (2×2) supercell with 1 ML on-surface fcc H atoms and one H atom placed initially at a on-surface hcp sites ($\theta_{\text{total}}=1.25$ ML), which is only possible channel for hydrogen penetration in this configuration. The hcp H atom is expected to incorporate downwards to the so-called tetraII sites in the first Mg interlayer, and the structure formed is noted as fcc/tetraII correspondingly. We found that there is no incorporation barriers exist for this process: H atom diffuses spontaneously downwards the subsurface tetraII sites. Actually, the zero barrier for H penetration was found at even lower on-surface H coverage of 0.75 ML [three fcc H atoms in (2×2) cell], in which the hcp atom was placed at the center of the three fcc H atoms. H penetration into the subsurface region via the hcp site surrounded by on-surface fcc H atoms offers an efficient channel for hydrogen absorption.

The absorption energies of resulted fcc/tetraII structures with increase in the subsurface tetraII H from 0.25 to 1.00 ML (see Table III) are: -0.23 eV/H ($\theta_{\text{total}}=1.25$ ML),

TABLE III. Calculated average absorption energies (eV) for the structures with 1 ML fcc or hcp H atoms on the surface ($\theta_{\text{on}}=1$ ML) and submonolayer subsurface octa, tetraI, and tetraII hydrogen ($\theta_{\text{sub}}=0.25, 0.50, 0.75$ and 1.00 ML), respectively. Corresponding total coverages (θ_{total}) are given at the bottom.

	Subsurface (θ_{sub})			
	0.25	0.50	0.75	1.00
	fcc ($\theta_{\text{on}}=1$ ML)			
octa	-0.10	-0.06	-0.05	-0.02
tetraI	-0.10	-0.03	0.04	0.10
tetraII	-0.23	-0.24	-0.24	-0.22
	hcp ($\theta_{\text{on}}=1$ ML)			
octa	-0.11	-0.11	-0.11	-0.09
tetraI	-0.03	0.03		0.12
tetraII	0.01			0.09
θ_{total}	1.25	1.50	1.75	2.00

-0.24 eV/H ($\theta_{\text{total}}=1.50$ ML), -0.24 eV/H ($\theta_{\text{total}}=1.75$ ML), and -0.22 eV/H ($\theta_{\text{total}}=2.00$ ML), respectively. For pure on-surface fcc H absorption at 1.00 ML, corresponding absorption energy is -0.19 eV/H. From these energetics, the differential binding energy for sequentially added first, second, third, and fourth tetraII H atom are -0.39, -0.29, -0.22, and -0.11 eV, respectively. Contrast to isolated subsurface H which is unstable or endothermic, these results show clearly that subsurface H is significantly stabilized by the presence of the on-surface H atoms, which facilitates the H penetration and absorption in the subsurface and bulk region.

The stabilization found above however does not exist for H atoms occupation at the octa and tetraI sites, as seen from corresponding differential binding energies are +0.25 eV (octa) and +0.25 eV (tetraI) (endothermic) for $\theta_{\text{sub}}=0.25$ ML (Table III). Significant destabilization comes from poor screening of the electrostatic repulsion between on-surface fcc H and subsurface octa H, where two H atoms face directly with each other [see Fig. 4(a)]. When subsurface H atoms absorb at the tetraII sites, a linear (fcc-H)-Mg-(tetraII-H) configuration forms, where Mg atom stands in the

middle and screen well the electrostatic repulsion between H atoms Fig. 4(c). The unique configuration is also favorable for the electronic hybridization, as discussed below.

When H atoms preabsorb and saturate at the hcp hollow sites, the absorption at the subsurface region were studied and the results are given in Table III. Contrast to on-surface H preabsorbed exclusively at the fcc sites, where the tetraII sites are energetically favorable, the absorption at the octa sites is energetically favorable than tetraI and tetraII sites. The resulted structure is schematically plotted in Fig. 4(b) and noted as hcp/octa. The preference for hcp/octa configuration is again from the favorable linear configuration formed between H atoms and Mg, as the fcc/tetraII one.

Fcc/tetraII and hcp/octa structures forms a similar H-Mg-H trilayer structure at overall absorption of $\theta_{\text{total}}=2$ ML, where surface Mg atoms coordinate with six H atoms (three above and three below) and stays in the center of H octahedrons. The difference between these two structures is the stacking consequence of the H-Mg-H trilayer with respect to the substrate underneath. The calculations show that the fcc/tetraII configuration is slightly favorable by 0.13 eV/H atom than hcp/octa configuration. This might come from the preference of H absorption at the on-surface fcc sites, as shown in Table I.

The energetics of the structures studied so far with presence of the subsurface H up to one monolayer is plotted in Fig. 2. Compared to the pure on-surface H absorption, it is found that for fcc/tetraII structures, average absorption energies are lowered roughly by 0.03 eV/H atom. Furthermore, the average absorption energies show a weak dependence on the coverage, and increases when $\theta > 1.50$ ML. These are unexpected because normally the incorporation of atoms into the interstitial sites will distort the lattice and raise the energy, correspondingly. To figure this out, we quantified the energy cost of the distortion, the distortion energy (E_{dis}), which is the difference of the total energy between predistorted Mg substrate induced by subsurface H and relaxed clean Mg substrate per (2×2) cell, and listed in Table IV with the variation in the first Mg interlayer spacing (Δd_{12})

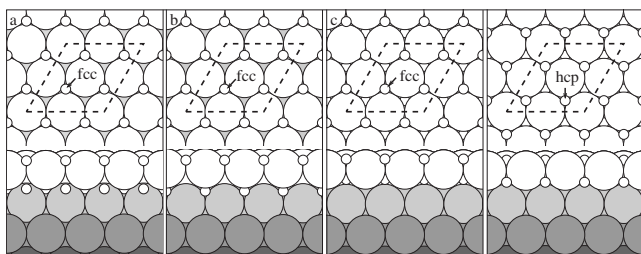


FIG. 4. The schematic model for the (a) fcc/octa, (b) fcc/tetraI, (c) fcc/tetraII, and (d) hcp/octa at $\theta_{\text{total}}=2$ ML, the upper parts are the top views and the lower parts are the side views. The gray gradient is used to denote the distance to surface, the lighter the closer to the surface. Small circles are H atoms, while big circles are Mg atoms. The dashed line shows the surface unit cell used in the calculation

TABLE IV. H absorption induced variation in the first Mg inter-layer spacing, Δd_{12} in percentage with respect to the bulk truncated value, and the distortion energy E_{dis} per (2×2) surface unit cell in eV.

$\theta_{total}(\theta_{on} + \theta_{sub})$ (ML)	Structure	Δd_{12} (%)	E_{dis} [eV/(2×2)]
1.00(1.00+0.00)	fcc	-1.6	0.01
1.25(1.00+0.25)	fcc/tetraII	0.8	0.01
1.50(1.00+0.50)	fcc/tetraII	2.9	0.01
1.75(1.00+0.75)	fcc/tetraII	5.9	0.05
2.00(1.00+1.00)	fcc/tetraII	9.7	0.12

with respect to the bulk truncated value. It is noted that for pure on-surface H absorption at 1 ML, Δd_{12} is -1.6% , and E_{dis} is 0.016 eV per (2×2) cell, namely, on-surface H absorption induced distortion is negligible. With incorporation of the subsurface H atoms, calculated Δd_{12} are 0.8% for $\theta_{sub}=0.25$ ML, 2.9% for $\theta_{sub}=0.50$ ML, 5.9% for $\theta_{sub}=0.75$ ML, and 9.7% for $\theta_{sub}=1.00$ ML, respectively. Corresponding E_{dis} becomes considerable only when the subsurface H absorption is larger than 0.50 ML. Compared to average absorption energy, the average distortion energies is 0.015 eV/H for the overall absorption of 2.00 ML, namely, the effect of the distortion to the overall energetics is modest.

After deducted the distortion energy from the average absorption energies for these mixed structures (with presence both of on-surface and subsurface H), the average binding energies from pure electronic interaction between H and Mg can be obtained. We found that the resulted binding energies are constant at the value of -0.205 eV/H for fcc/tetraII configuration at $\theta=2$ ML, compared to -0.190 eV/H for pure on-surface fcc H at 1 ML. This indicates that Mg(0001) tends to accommodate H atoms by forming H-Mg-H trilayer without being to be destabilized, which is good for improving the energetics for H uptake. The stabilization to form this H-Mg-H trilayer structures can be rationalized from the enhanced orbital hybridization between H and Mg, which can be seen from corresponding projected DOS as plotted in Fig. 5. When the subsurface H absorptions are lower ($\theta_{sub}=0.25$ ML and $\theta_{total}=1.25$ ML), the hybridization with surface Mg atoms occurs mainly at low lying energy [-7 eV, Fig. 5(a)], while on-surface H atoms prevail mainly at high lying energies. With increase in the subsurface H absorption, its interaction with surface Mg atoms at high lying energies (-4 eV) increases. Meanwhile, PDOS for on-surface H atoms changes accordingly, which indicates the interaction between subsurface and on-surface H atoms through Mg atoms in between. The interaction is maximized when the subsurface H absorption approaches 1 ML, as plotted in Fig. 5(d), where the PDOS for the subsurface and on-surface H atoms looks similar. This is understandable because from surface Mg layer point of view: both the subsurface and on-surface H atoms share same Mg layer: absorb at threefold hollow sites and form a 1 ML structure, which are energetically favorable as found in pure on-surface H absorption above. Correspondingly, the overall energetics of the system is improved. The interaction mediated through surface Mg layer,

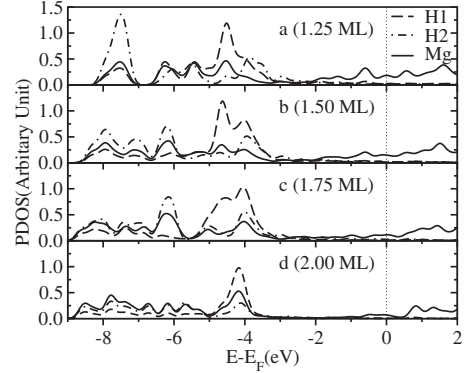


FIG. 5. PDOS for on-surface fcc H atom (H1, dash-dot-dash line) and subsurface tetraII H atom (H2, dash-dot-dot-dash line) and surface Mg atoms (solid line) for fcc/tetraII configuration at overall absorption of (a) 1.25, (b) 1.5, (c) 1.75, and (d) 2 ML, respectively.

on-surface and subsurface H also indicates that the coupling between the H-Mg-H trilayer formed and Mg atoms underneath may be weakened. Otherwise the interaction between the subsurface H and the Mg atoms underneath would change subsurface H PDOS, which is clearly not the case, as seen from Fig. 5(d). The weakened coupling between H-Mg-H trilayer may facilitate the hydrogen uptake and formation of Mg hydride, which would be discussed below.

V. FORMATION OF MULTITRILAYERS AND TRANSITION TO Mg HYDRIDE

A. Formation of multitrilayer

After the formation of H-Mg-H trilayer with overall absorption of 2 ML H, further H absorption was studied. In this case, coming H atoms may absorb either in the remained sites in the first Mg interlayer, or the interstitial sites in the second Mg interlayer. For fcc/tetraII (2 ML) structure discussed above, for instance, we found that for coming 0.25 ML H atoms, corresponding absorption energy is -0.12 eV (tetraI) and -0.21 eV (octa) for H in the first Mg interlayer and -0.06 eV (tetraI) for H in the second Mg interlayer. This holds true for coming additional H up to full monolayer. These indicates clearly that on fcc/tetraII H-Mg-H trilayer, coming H atoms would tend to absorb at the available (octa) sites in the 1st Mg interlayer and form a 3 ML structure (noted as fcc/tetraII-octa), instead of absorption at the deeper region.

Looking at the geometry of fcc/tetraII-octa configuration, it is found that the first Mg interlayer spacing increases from 2.58 Å for bulk truncated interlayer spacing of Mg (0001) surface to 3.17 Å, meanwhile calculated interlayer spacing between the second and third H layer is 1.65 Å. With such a considerable separation, it is expected that the coupling between H-Mg-H trilayer and the substrates underneath is significantly weakened. To test this, we have calculated decoupling energy of lifting off the outmost Mg layer from clean surface, H-Mg-H trilayer with total H absorption of 2 ML (fcc/tetraII) and 3 ML (fcc/tetraII-octa), as schematically shown in Fig. 6. From the figure, it is seen that to lift off the outmost Mg layer from clean Mg surface, 0.62 eV/Mg atom

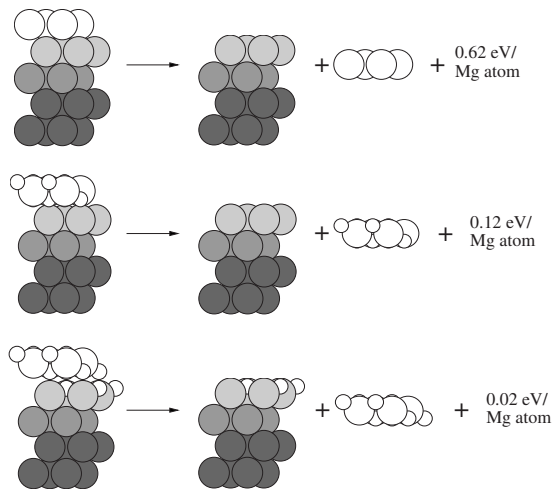


FIG. 6. Energy (per Mg atom) required to lift off a complete Mg layer from (a) Mg(0001) substrate underneath for clean surface, (b) for H-Mg-H (fcc/tetraII) trilayer with $\theta_{\text{total}}=2$ ML, and (c) for fcc/tetraII-octa configuration with $\theta_{\text{total}}=3$ ML. The big circles represent Mg atoms and the small circles represent H atoms. The gray gradient shows how far the atoms are from the surface.

is needed; when H-Mg-H (fcc/tetraII) trilayer is formed, the energy cost decreases dramatically to 0.12 eV/Mg atom. While for fcc/tetraII-octa configuration, in which there is 1ML H between the H-Mg-H trilayer and the second Mg layer, corresponding decoupling energies becomes negligible (less than 0.02 eV/Mg atom). These show clearly that the H-Mg-H trilayer could be a stable locale structure with weak coupling to the substrates underneath while strongly bound inside itself, which may facilitate further hydrogenation of Mg substrate, correspondingly.

The weak coupling of the H-Mg-H trilayer with the substrate underneath can also be visualized from PDOS. From Fig. 7(a), it can be found that PDOS for H-Mg-H trilayer are close, independent on if it sits on the Mg substrates or H-covered Mg substrates. Furthermore, the PDOS [Fig. 7(b)] for the third H (octa) layer is similar to the pure on-surface H (fcc) absorption at 1 ML [Fig. 3(e)]. The similarity and weak coupling between H-Mg-H trilayer and substrates underneath

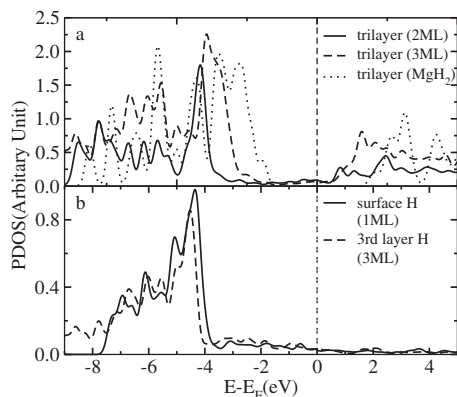


FIG. 7. PDOS of H-Mg-H trilayers with coverage of 2, 3, and (a) in rutile MgH_2 , and of surface H with coverage of 1 ML and (b) the third H layer where the total coverage is 3 ML.

indicate that the third H layer bonds stronger with the Mg substrate underneath, instead of above H-Mg-H trilayer.

The above analysis suggests that further absorption in deep Mg region may repeat the absorption in the surface Mg region. Our calculations do show that further incorporation of H atoms prefers to absorb the sites in deeper Mg interlayer region, specifically, the tetraII sites in the second Mg interlayer, and forms a second H-Mg-H trilayer. The calculated average absorption energy of resulted two H-Mg-H trilayers is -0.21 eV/H, compared to the single H-Mg-H trilayer of -0.22 eV/H.

B. Transition toward Mg hydride

Preference of the formation of two H-Mg-H trilayer found above comes from the stable locale H-Mg-H trilayer and weak coupling in between. The whole process can be repeated and a stacking of multitrilayer is expected, which may end up with a phase transition toward the bulk hydride MgH_2 . Indeed, calculated multi H-Mg-H layers show already some characteristics of MgH_2 . Bulk MgH_2 has a rutile-like structure, where Mg atoms stay in the center of H octahedron and coordinate with six H atoms around. This is also found in H-Mg-H trilayer. Furthermore, both of H-Mg-H multitrilayer and rutile MgH_2 present similar electronic properties. In Fig. 7(a), the PDOS for bulk MgH_2 are plotted. It can be found that there is a band gap (3 eV) opening, which indicates that bulk MgH_2 is an insulator. While for single H-Mg-H trilayer with $\theta_{\text{total}}=3$ ML, a slightly smaller band gap (around 2 eV) can be found. Overall feature between rutile and H-Mg-H trilayer PDOSs are close, though MgH_2 PDOS is sharper. The sharpness and enhanced hybridization for the previous one indicate the stronger interaction between H and Mg in MgH_2 , which is inline with larger calculated heat of formation of Mg hydride (-0.32 eV/H atom) than the average absorption energy of two H-Mg-H trilayer on Mg substrate (-0.207 eV/H atom and $\theta_{\text{total}}=4$ ML).

To study the transition from the multi H-Mg-H trilayer to the Mg hydride and identify the point to which phase transition may occur, the average absorption energy of a free-standing stack of H-Mg-H trilayer and rutile $\text{MgH}_2(110)$ layer (in same stoichiometries) at various thickness were calculated and plotted in Fig. 8. As an approximation, the coupling with the substrates underneath is neglected, which nevertheless is small as discussed above for the H-Mg-H trilayer. For stacking of the $\text{MgH}_2(110)$ layer, though the interaction with the substrates underneath is unclear and may not be negligible, we note that the interfacial interaction will become less important with increase in the number layers, since its proportion with respect to the overall energy gain decreases gradually. From Fig. 8, it can be found that the growth of multi H-Mg-H trilayers is more or less independent on the number of layers, as expected because of its weak interlayer coupling, and converges eventually at -0.17 eV/H. For free-standing rutile layer, as indicated in Fig. 8 inset, hydrogen atoms stick out of the film and act as the links between Mg layers. At the beginning of the growth of the rutile layer, rutile layer is energetically unfavorable due to the dangling Mg-H bond. However, its energetics

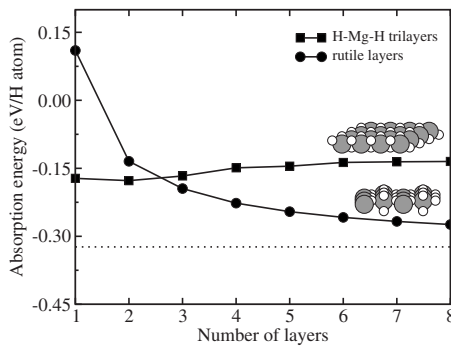


FIG. 8. Average absorption energies of H-Mg-H trilayers (square) and $\text{MgH}_2(110)$ orientated rutile layers (circle) as a function of numbers of layers in the stack. The dotted line indicates the calculated formation energy of bulk MgH_2 , which is the limit approached by the rutile curve for the infinite thick slab.

drops significantly with increase in the number of layers by forming bond between (110) orientated rutile layers, and gradually approaches the limit of -0.32 eV, the formation energy of bulk rutile MgH_2 . From Fig. 8, it is seen that at three H-Mg-H trilayer, the stacking of rutile layers becomes energetically more favorable. This means that as long as this point is reached, given proper temperature, stacking of H-Mg-H trilayers would transform to rutile MgH_2 .

These analyses lead us to propose that H-Mg-H trilayers found in present work is a kind of “surface hydride,” which shares some geometric and electronic features of the Mg hydride. It may act as the precursor for the transition to Mg hydride with increase in H absorption. Furthermore, we note that the transition may be prevented by kinetics, where the massive transportation are required. In literatures, similar process has been found for oxidation of Ru(0001) (Ref. 34) and Ag(111).^{35–37} For the previous one, O-Ru-O trilayer has been identified and forms eventually the rutile $\text{RuO}_2(110)$ surface after severe oxidation at elevated temperatures. Interestingly, an accordion like unfolding mechanism for the transition from the O-Ru-O trilayer to RuO_2 is proposed, which may be applied to the present work.

The present calculations show that with increase in the absorption, H atoms prefer to adsorb at the fcc hollow sites. After saturating on-surface fcc hollow sites, coming H atoms penetrate to the subsurface region through the hcp channel with zero barrier, and a H-Mg-H trilayer is formed. Though the H-Mg-H trilayers may stack sequentially and transit to bulk MgH_2 as discussed above, we note that within H-Mg-H

trilayer, the channel for H incorporation is blocked either by on-surface fcc H or subsurface tetraH. In other words, the dense H-Mg-H trilayer may block the diffusion channel, and slow down the kinetics of the H absorption, correspondingly. Indeed, this was observed by recent experiments.¹⁰ For Mg films grown on molybdenum, Ostenfeld *et al.*³⁸ found that the rate of hydrogen uptake decreases with time, and the total amount of the uptake saturates at about 2.5 ML in 50 min when temperature is lower than 423 K. The reason was attributed to the formation of dense hydrogen overlayer, which was supported by the present calculations. Experiments however suggest that the uptake rate can be improved significantly by doping Pt catalysts,^{10,11} which was proposed to decrease the influence of self blocking caused by hydrogen adsorbed on the surfaces. Another possibility to improve the kinetics for H absorption is use of Mg nanoparticles. The nanoparticles expose itself with various facets and defects, which may facilitate the hydrogen uptake, besides short diffusion path into the bulk.^{9,22}

VI. CONCLUSION

The absorption of H on Mg (0001) surface up to 6 ML is studied by density-functional theory calculations and valuable insights have been obtained. It is found that for H absorption on Mg(0001) surfaces, the H absorption is exothermic and H prefers to the fcc hollow sites. The bonding energies increase with the absorption up to 1 ML due to the enhanced hybridization between H and Mg substrates. Our calculations show that the H absorption in the subsurface region is energetically unfavorable at lower absorption. However, it becomes energetically and kinetically favorable via the hcp channel with further increase in the absorption. We find a stable locale H-Mg-H trilayer (surface hydride), a precursor state for Mg hydride. Formation of H-Mg-H trilayer can be repeated and form a stacking of H-Mg-H trilayers. It is found that when the number of trilayers is over three, the formation of $\text{MgH}_2(110)$ would be energetically favorable.

ACKNOWLEDGMENTS

We thank the Natural Science Foundation of China (Grants No. 20873142, No. 20733008, No. 2083309, No. 20873148, No. 50671098, and No. U0734005) and National Basic Research Program of China (Grant No. 2010CB631303) for financial support.

*Corresponding author; wxli@dicp.ac.cn

¹http://www.eere.energy.gov.

²L. Schlappach and A. Züttel, *Nature (London)* **414**, 353 (2001).

³R. B. Schwarz, *MRS Bull.* **24**, 40 (1999).

⁴J. L. Bobet, B. Chevalier, and B. Darriet, *J. Alloys Compd.* **330-332**, 738 (2002).

⁵S. Rivoirard, P. de Rango, D. Fruchart, J. Charbonnier, and D. Vempaire, *J. Alloys Compd.* **356-357**, 622 (2003).

⁶G. Liang, *J. Alloys Compd.* **370**, 123 (2004).

⁷C. Z. Wu, P. Wang, X. D. Yao, C. Liu, D. M. Chen, G. Q. Lu, and H. M. Cheng, *J. Phys. Chem. B* **109**, 22217 (2005).

⁸N. Gerad and S. Ono, *Hydrogen in Intermetallic Compounds II. Topics in Applied Physics* (Springer, Berlin, 1992), Vol. 67.

⁹N. Hanada, T. Ichikawa, and H. Fujii, *J. Phys. Chem. B* **109**, 7188 (2005).

¹⁰C. W. Ostenfeld, M. Johansson, and I. Chorkendorff, *Surf. Sci.*

- 601**, 1862 (2007).
- ¹¹M. Johansson, C. W. Ostefeld, and I. Chorkendorff, *Phys. Rev. B* **74**, 193408 (2006).
- ¹²P. T. Sprunger and E. W. Plummer, *Chem. Phys. Lett.* **187**, 559 (1991).
- ¹³P. T. Sprunger and E. W. Plummer, *Surf. Sci.* **307-309**, 118 (1994).
- ¹⁴K. Higuchi, K. Yamamoto, H. Kajioka, K. Toiyama, M. Honda, S. Orimo, and H. Fujii, *J. Alloys Compd.* **330-332**, 526 (2002).
- ¹⁵J. K. Nørskov, A. Houmøller, P. K. Johansson, and B. I. Lundqvist, *Phys. Rev. Lett.* **46**, 257 (1981).
- ¹⁶T. Vegge, *Phys. Rev. B* **70**, 035412 (2004).
- ¹⁷B. Hammer, L. B. Hansen, and J. K. Nørskov, *Phys. Rev. B* **59**, 7413 (1999).
- ¹⁸N. Jacobson, B. Tegner, E. Schröder, P. Hyltdgaard, and B. I. Lundqvist, *Comput. Mater. Sci.* **24**, 273 (2002).
- ¹⁹G. X. Wu, J. Y. Zhang, Y. Q. Wu, Q. Li, K. C. Chou, X. H. Bao, and G. Q. Lu, *Acta Phys. Chim. Debrecina* **24**, 55 (2008).
- ²⁰A. J. Du, S. C. Smith, X. D. Yao, and G. Q. Lu, *J. Phys. Chem. B* **109**, 18037 (2005).
- ²¹A. J. Du, S. C. Smith, X. D. Yao, and G. Q. Lu, *J. Phys. Chem. B* **110**, 1814 (2006).
- ²²R. Wagemans, J. vanLenthe, P. deJongh, A. vanDillen, and K. de-Jong, *J. Am. Chem. Soc.* **127**, 16675 (2005).
- ²³D. Vanderbilt, *Phys. Rev. B* **41**, 7892 (1990).
- ²⁴J. Neugebauer and M. Scheffler, *Phys. Rev. B* **46**, 16067 (1992).
- ²⁵H. J. Monkhorst and J. D. Pack, *Phys. Rev. B* **13**, 5188 (1976).
- ²⁶J. L. F. Da Silva, C. Stampfl, and M. Scheffler, *Surf. Sci.* **600**, 703 (2006).
- ²⁷C. Kittel, *Introduction to Solid State Physics*, 7th ed. (Wiley, New York, 1996).
- ²⁸F. R. D. Boer, R. Boom, W. C. M. Mattens, A. R. Miedema, and A. K. Niessen, *Cohesion in Metals* (Elsevier, North-Holland, Amsterdam, 1988).
- ²⁹W. Kohn, *Rev. Mod. Phys.* **71**, 1253 (1999).
- ³⁰J. J. Liang, *Appl. Phys. A: Mater. Sci. Process.* **80**, 173 (2005).
- ³¹H. J. Gotsis, D. A. Papaconstantopoulos, and M. J. Mehl, *Phys. Rev. B* **65**, 134101 (2002).
- ³²I. Baraille, C. Pouchan, M. Causà, and F. Marinelli, *J. Phys.: Condens. Matter* **10**, 10969 (1998).
- ³³X. G. Li, P. Zhang, and C. K. Chan, *Physica B* **390**, 225 (2007).
- ³⁴K. Reuter, M. V. Ganduglia-Pirovano, C. Stampfl, and M. Scheffler, *Phys. Rev. B* **65**, 165403 (2002).
- ³⁵W. X. Li, C. Stampfl, and M. Scheffler, *Phys. Rev. B* **65**, 075407 (2002).
- ³⁶W. X. Li, C. Stampfl, and M. Scheffler, *Phys. Rev. B* **67**, 045408 (2003).
- ³⁷W. X. Li, C. Stampfl, and M. Scheffler, *Phys. Rev. B* **68**, 165412 (2003).
- ³⁸C. W. Ostefeld, J. C. Davies, T. Vegge, and I. Chorkendorff, *Surf. Sci.* **584**, 17 (2005).